Kondepu, K., Sgambelluri, A., Sambo, N., Giannone, F., Castoldi, P. y Valcarenghi, L. (2018). Orchestrating Lightpath Recovery and Flexible Functional Split to Preserve Virtualized RAN Connectivity. *Journal of Optical Communications and Networking*, 10 (11), pp. 843-851.

DOI: https://doi.org/10.1364/JOCN.10.000843

Orchestrating lightpath recovery and flexible functional split to preserve virtualized RAN connectivity

K. Kondepu, A. Sgambelluri, N. Sambo, F. Giannone, P. Castoldi, L. Valcarenghi

***Abstract*—In the Next Generation Radio Access Network (NG RAN), the next generation eNBs (gNBs) will be, likely, split into virtualized Central Units (CUs) and Distributed Units (DUs) interconnected by a fronthaul network. Because of the fronthaul latency and capacity requirements, optical metro ring networks are among the main candidates for supporting converged 5G and non-5G services.**

In this scenario, a degradation in the quality of transmission of the lightpaths connecting DU and CU can be revealed (or anticipated) based on monitoring techniques. Thus, the lightpath transmission parameters can be adapted to maintain the required bit error rate (BER). However, in specific cases, the original requested capacity between DU and CU could be not guaranteed, thus impacting the service. In this case, another DU-CU connectivity should be considered, relying to a change of the so called functional split.

This study proposes a two-step recovery scheme orchestrating lightpath transmission adaptation and functional split reconfiguration to guarantee the requested connectivity in a Virtulized RAN fronthaul. Results show that for the connections that cannot be transported by the original lightpath a graceful degradation followed by a recovery is possible within tens of seconds.

***Index Terms*—flexible functional split; recovery; lightpath transmission adaptation.**

I. Introduction

In the coming years, the establishment of 5G technology will impact the design, the control, and the management of metro networks [1]–[3]. The dimensioning of metro rings will be driven by the maximum latency admitted by 5G services and verticals. The network capacity will increase to support several high-bandwidth fronthaul/backhaul connections. Thus, the employment of transponders based on high-spectral efficient multi-level modulation formats (e.g., polarization multiplexing 16 quadrature amplitude modulation — PM-16QAM) are expected to penetrate this market. Moreover, proper programmability and control of transmission systems and switching will enable dynamic provisioning of connectivity and its survivability. At the same time, operators, European Community, and researchers are working to reduce CAPEX (e.g., by a factor of ten) and OPEX to make the network more scalable [2], [4].

On the one hand, a way considered by operators and vendors to reduce the costs of an optical network is the reduction of margins [5]. Indeed, margins to the quality of transmission are typically adopted to consider uncertainties of physical layer models and device aging. This is a pessimistic but conservative approach that enables uninterrupted service of connections during the whole life of the network but that could also bring to the overestimation of the number of regenerators, in turn of costs. Reducing margins can decrease costs (e.g., of regenerators) but can also increase the probability of experiencing soft failures [6] (i.e., degradations of the connectivity resulting in bit error rate (BER) increase over the acceptable thresholds) due to model uncertainties and ageing. Differently from hard failures (e.g., link cut), where only re-routing enables traffic recovery, soft failures can be also overcome by adopting a more robust transmission along the degraded path, for example by adapting the modulation format (e.g., changing from PM-16QAM to the more robust polarization multiplexing quadrature phase shift keying —PM-QPSK) or by increasing the code redundancy. Hereafter, "lightpath adaptation" refers to operations involving the change of transmission settings of a lightpath, as the adaptation of the modulation format, of the rate, or of the code redundancy. Lightpath adaptation can be particularly fast and, in some cases, hitless [7] (e.g., change of rate).

However, modulation format change or code redundancy increase at fixed baud rate implies an information rate reduction [6]. Thus, if recovery is performed through modulation format or code adaptation, part of the traffic can be promptly recovered along the same path, while other has to be re-routed or, alternatively, suppressed if the service class admits a bit rate reduction [6], [8].

On the other hand, another way to reduce costs is resorting to network function virtualisation. Indeed, the 5G network is expected to be heavily based on virtual network functions (VNFs) representing "a transition from today's *network of entities* to a *network of (virtual) functions*" [9]. Network function virtualization (NFV) enables an easy introduction of new network ser-

K. Kondepu (email: k.kondepu@santannapisa.it), A. Sgambelluri, N. Sambo, P. Castoldi, and L. Valcarenghi are with Scuola Superiore Sant'Anna, Pisa, Italy.

vices by adding dynamic programmability to network devices (e.g., as routers, switches, and applications servers) that, in turn, empowers fast, flexible, and dynamic deployment of new network and management services. The exploitation of NFV is foreseen also in the Next Generation Radio Access Network (NG RAN) architecture supporting the New Radio (NR) access technology [10] and paving the way to the virtual RAN (vRAN) [11]. In the NG RAN the evolved NodeB (eNB) functions are split into two new, most likely virtualized, network entities [12]: the Central Unit (CU) deployed in centralised locations and the Distributed Unit (DU) deployed near the antenna. Several *functional splits* are being considered by 3GPP in TR 38.801 [12], IEEE 1914 Working Group in Next Generation Fronthaul Interface (NGFI) [13], and in the Common Public Radio Interface eCPRI Specification [14]. They demand different requirements in terms of latency and capacity to the fronthaul network connecting DU and CU [15] and discussion on which split option shall be supported is still ongoing [16].

Therefore, it is expected that a metro network will carry a converged mix of traffic including fronthaul, backhaul, and non mobile traffic, requiring large capacity. In this scenario, guaranteeing reliability is of paramount importance. The failure scenarios can be several (i.e., virtual machine/container failure, optical link failure, etc.) but this paper focuses on the failure of the fronthaul connection carrying the virtual link between a virtualized DU (vDU) and a virtualized CU (vCU).

In particular, a lightpath, which carries the frontahul connection, soft-failure (i.e., a degradation of the quality of transmission) is considered. In this scenario, upon a failure, the connectivity between vDUs and vCUs can be easily recovered by changing the modulation format or increasing the code redundancy. However, the consequent rate/capacity reduction might not be acceptable by the fronthaul, implying the re-routing of the original lightpath along a different route. Nevertheless, such re-routing might fail if the available capacity on the other direction of the ring is not sufficient.

This paper presents and evaluates a two-step recovery scheme, stemming from the one presented in [17], orchestrating lightpath adaptation and eNB functional split reconfiguration to recover the vDU-vCU connectivity while fulfilling the fronthaul capacity requirements. Although resilient schemes for recovering failures when network functions are virtualized have been already investigated [18] or can be based on previous research on cloud [19] and grid computing [20], the originality of the proposed scheme consists in exploiting functional split flexibility to improve vRAN reliability. The scheme first recovers the soft failure by lightpath adaptation or lightpath rerouting (the introduction of lightpath rerouting represents the main difference with respect to [17]) and, if the provided capacity is not sufficient, it modifies the functional split between vDUs and vCUs so that it can be supported by the new lightpath capacity.

The results, collected via simulation and experimental evaluation, show that, at the beginning, the vDU-vCU virtual link incurs a graceful degradation due to lightpath adaptation. Then, upon functional split reconfiguration, the vDU-vCU virtual link is recovered to fully support the required capacity. The overall recovery time is in the order of few seconds if several vDU and vCU functional splits are pre-deployed.

II. Scenario and two-step recovery scheme

This section summarizes the considered scenario and the proposed two-step recovery scheme. The city of Milan is considered as a sample metropolitan city. The city metropolitan area covers about two-hundred square kilometers. By assuming an antenna density of one antenna per two square kilometers, one hundred antenna sites provides connectivity to the entire area. If split option 2 is utilized as functional split, the capacity required by the connections between DU and CU is about 4 Gb/s in each direction, as reported in Tab. I from 3GPP TR 38.801. This connection can be supported by a 10 GbE link between DU and CU. By multiplying each antenna fronthaul requirement by the number of antenna sites the overall required capacity sums up to 1 Tb/s as summarized in Tab. II.

Based on the data reported above and on practical deployment considerations [21] the architecture depicted in Fig. 1 is considered. Antenna sites are connected to optical switches that form an optical metro ring network. The network architecture connecting the antenna site and metro ring switch can be several; two possible solutions are point to point connections or next generation passive optical network (NG-PON2). DUs and CUs are virtualized. vDUs are placed either at the antenna sites or in their vicinity (connected to the same metro switch). vCUs are placed in another data center connected to one of the metro ring switches. The connectivity between vCU and vDU is implemented by means of lightpaths routed in the optical metro ring network with 8 km radius. Such radius implies a circumference of about 50 km with a maximum latency of about 250 s (considering propagation delay only).

The proposed scheme is implemented in the architecture depicted in Fig. 1 that is, in turn, derived from the ETSI NFV-MANO architecture [22]. The Network Function Virtualization Orchestrator (NFVO) is responsible for orchestrating vDU, vCU, and network resources and for selecting the proper functional split. The Virtual Infrastructure Manager (VIM)/Virtual Network Function Manager (VNFM) are responsible for provisioning the required compute, storage, and network resources and deploying vDU and the vCU according to the functional split selected by NFVO.

Table I
FRONTHAUL REQUIREMENTS.

Split option	Required bandwidth	Max. allowed one way latency [time]
Option 2	DL: 4Gb/s; UL: 3Gb/s	10ms
Option 7a	DL: 10.1∼22.2Gb/s; UL: 16.6∼21.6Gb/s	250μs
Option 7b	DL: 37.8∼86.1Gb/s; UL: 53.8∼86.1Gb/s	250μs
Option 7c	DL: 10.1∼22.2Gb/s; UL: 53.8∼86.1Gb/s	250μs
Option 8	DL: 157.3Gb/s; UL: 157.3Gb/s	250μs

Table II
METROPOLITAN AREA CAPACITY REQUIREMENTS.

City	Milan, Italy
Metropolitan area	200 km^2
Number of antenna sites	100
Average antenna density	0.5 km $^{-2}$
Functional split	Option 2
Required capacity per antenna site	4Gb/s per direction (UL/DL)
Overall fronthaul required capacity	1Tb/s

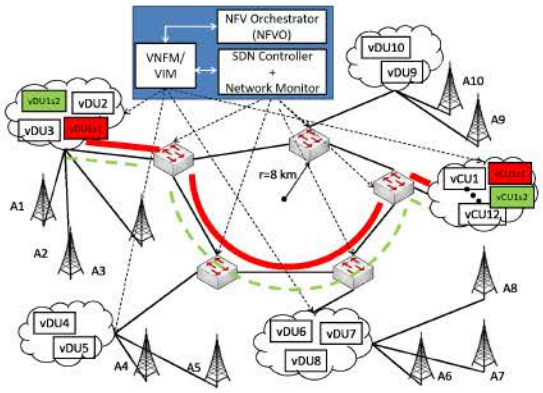

Figure 1. Metro fronthaul architecture

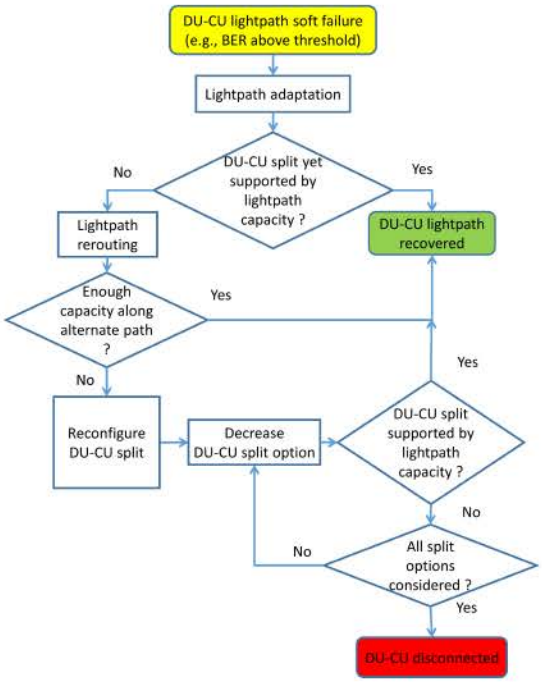

Figure 2. Two-step recovery scheme flow chart

The SDN controller is responsible for the control of vDU-vCU connectivity, thus for the configuration of the optical metro segment. The SDN controller is enhanced with a Network Monitor, monitoring the lightpath status.

Fig. 2 shows the flow chart of the proposed two-step recovery scheme. Upon detection of a soft failure, lightpath adaptation is triggered. Lightpath adaptation is performed by the SDN controller, which configures transmitter and receiver with the new configuration settings. Lightpath adaptation can be based on modulation format adaptation, which can be performed by a digital-to-analog converter (DAC), typically employed in transponders based on coherent transmission, now expected to penetrate also the metro network market [23]. Upon adaptation, if the functional split rate is still supported by the lightpath, the original functional

split is recovered and maintained. Otherwise, another path is searched to recover the original rate (this step is not present in [17]). If no path is found or, more in general, the functional split cannot be supported, the functional split reconfiguration is triggered. A functional split is sought starting from the highest split option (i.e., lowest functional layer split) that could be carried by the adapted lightpath (this step is not present in [17]). In case of success the vDU-vCU connectivity is recovered. Otherwise, it is lost. The decision to start the search from the highest split option is to minimize the degradation on the wireless transmission performance.

As an example, the working lightpath (red solid line in Fig. 1) connecting vDU and vCU is monitored by the Network Monitor. Such monitor reveals or even anticipates degradation in the quality of transmission of the working lightpath and it notifies the SDN controller, which triggers the modification of the lightpath modulation format or the code redundancy increase (i.e., green dashed line) if needed. If the resulting lightpath rate is not capable of carrying the original functional split (i.e., vDU1s1 and vCU1s1), the SDN controller attempts to establish another lightpath along the opposite direction of the ring. If unsuccessful, the NFVO is notified and it triggers the modification of the functional split to one requesting a lower data rate (i.e., vDU1s2 and vCU1s2) and the vDU-vCU connectivity is recovered along the original path with an adapted lightpath.

III. Performance evaluation parameters and scenario

A. Simulation scenario

Simulations are carried out to evaluate the amount of fronthaul interfaces that can be recovered through transmission parameter adaptation (thus, without re-routing) in a metro network. A custom built event-driven C++ simulator is utilized and a five-node ring topology is considered. Each link is 10 km long, not needing in-line amplifiers. Optical amplifiers are assumed as boosters. In the metro network, connection requests, aggregating 5G services, are modelled as a Poisson process (e.g., emulating a small cell on-off process). The holding time of each connection is exponentially distributed with average $1/\mu = 5000$ s. The traffic load offered to the network is expressed as λ/μ, where $1/\lambda$ is the mean inter-arrival time of connections requests. Transponders supporting 200 Gb/s PM-16QAM and 100 Gb/s PM-QPSK are considered. The bit error rate (BER) of both PM-16QAM and PM-QPSK is computed through the optical signal to noise ratio (OSNR) and assuming negligible non-linear effects given the limited distances of the metro network [24]–[26]. A BER lower than 10^{-3} is assumed as acceptable. In particular, 200 Gb/s PM-16QAM is considered acceptable with an OSNR higher than 20.5 dB, while the model in [26] is adopted for 100 Gb/s PM-QPSK. Soft failures are randomly generated on a single link. We assume that a 200 Gb/s lightpath carries an aggregation of Option 8 functional split traffic, while a 100 Gb/s lightpath carries an aggregation of Option 7 functional split traffic. It is assumed that Option 8 and Option 7 fronthaul interfaces require 253 Mb/s and 160 Mb/s, respectively, such values were obtained experimentally by using OAI as in [27]. Thus, a 200 Gb/s lightpath carries around 790 Option-8 fronthaul interfaces, while while a 100 Gb/s around 625 Option 7 fronthaul interfaces. The proposed two-step recovery scheme is compared with re-routing. When re-routing is applied, if a lightpath is impacted by the soft failure (BER above the threshold), re-routing is performed while keeping unchanged 200Gb/s (and modulation format), thus unchanged Option 8. Two-step recovery and re-routing are compared in terms of supported fronthaul interfaces after the soft failure. Results are recorded until the confidence interval of 5% at 95% confidence level is achieved.

B. Experimental scenario

The considered experimental evaluation scenario is shown in Fig. 3. Here, the Evolved Packet Core (EPC) is deployed in *Host Machine 1*, CUs, DUs are virtualised in *Host Machine 2* and *Host Machine 3*, respectively. In particular, the EPC contains three different components that are running in the *Host Machine 1* such as Mobile Management Entity (MME), Home Subscriber Server (HSS) and Serving and Packet Gateway (SPGW). An open source software (*openair-cn*) from the OpenAirInterface (OAI) [28] is utilized as EPC [29]. It implements the EPC 3GPP specifications with all the specified EPC components. The functional splits implemented by the OAI platform and considered in this paper are the IF5 and IF4.5, namely Option 8 and Option 7a in the 3GPP terminology [12]. Specifically, if split Option 8 is considered baseband signal I/Q time-domain samples are transmitted from the vDU to the vCU that implements all the LTE-A protocol stack functions. If Option 7a is considered frequency domain samples are transmitted instead.

The fronthaul link between vCU and vDU is assumed to be realized by means of an optical metro-network including sliceable transponders capable to adapt the modulation format and the spectrum occupation according to the required bit-rate and path length. The transmitters (TXs) support different modulation formats (i.e., QPSK, 8QAM, 16QAM) and different baudrate (i.e., 28Gbaud and 32Gbaud in relation to the Forward Error Correction—FEC code rate adopted). Optical data plane is emulated considering BER values collected through measurements in the setup described by [30]. Each node is equipped with a Network Configuration Protocol (NETCONF) agent, developed using ConfD framework, in order to enable

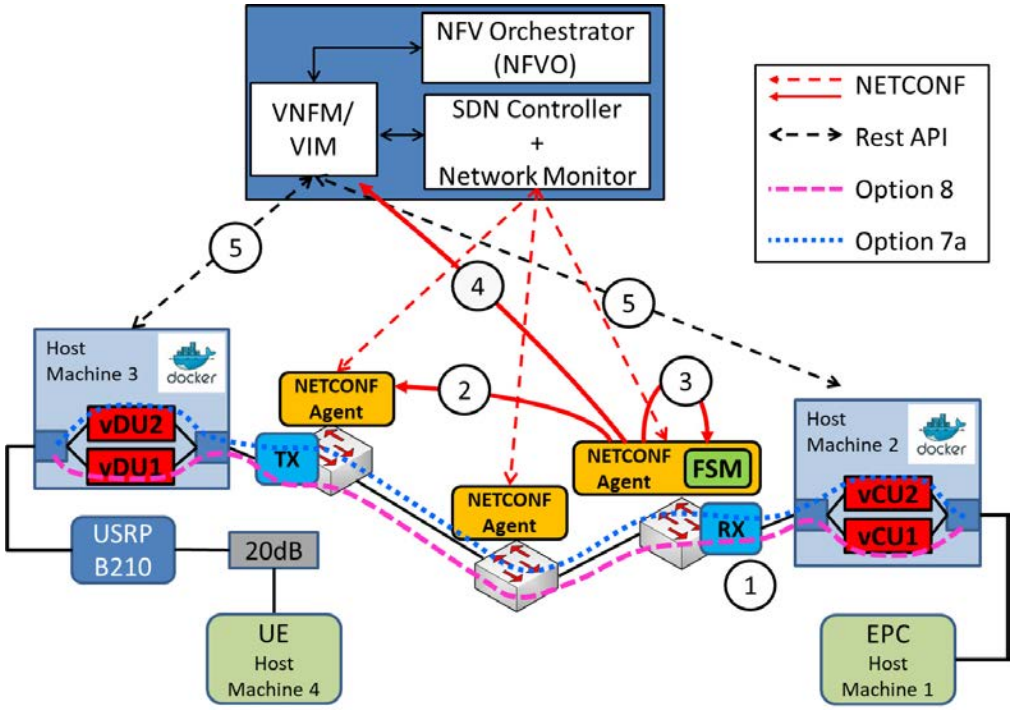

Figure 3. Scenario considered for the experimental evaluation

the SDN paradigm. The SDN Controller relies on NETCONF protocol to perform the configuration and the monitoring of Optical nodes. By mean of NETCONF `edit-config`, the SDN controller configures the traversed ROADMS and the considered transponders.

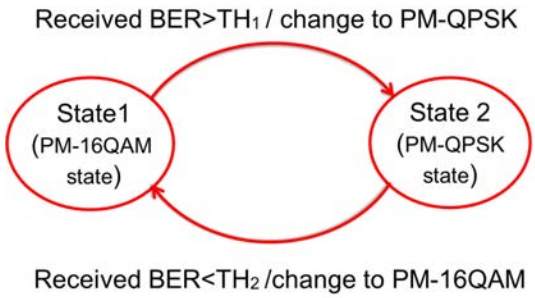

Figure 4. Lightpath transmission adaptation FSM

When a lightpath is configured, the receiver periodically reports monitored parameters, including pre-FEC, BER, and OSNR. All the receiver transponders are configured with specific Finite Stete Machines (FSMs), in order to automatically adapt the lightpath transmission rate in case of known events. The considered FSM is shown in Fig. 4. As an example, if the lightpath operates at "State 1" but the BER exceeds a threshold, modulation format adaptation is triggered and the transition to "State 2" is performed. Reversely, if the lightpath operates at "State 2" but the BER is below a threshold, modulation format adaptation is triggered and the transition to "State 1" is performed.

In our experiments, to perform modulation format adaptation, we exploited the scheme proposed in [31], [32] based on FSM for enabling fast reconfiguration. In this way, if the value of BER monitored at the receiver exceeds the configured threshold, the automatic reconfiguration of TX and RX can be performed locally without involving the SDN controller. The portion of the FSM (State 1) to be adopted for the automatic reconfiguration in case of monitored BER greater than 0.002 is shown in Fig. 5. A similar configuration file (not reported) is utilized for the transition to State 2. The reconfiguration consists in adapting the lightpath with a baudrate of 28Gbauds and a more robust modulation-format (i.e., PM-QPSK) at both the TX (remote agent) and the RX (local agent). The FSM presents another state (i.e., State2, not shown in figure), designed for the case when the value of BER undergoes the threshold of 0.00004. In fact, in this occurrence, the lightpath is reconfigured with a baudrate of 32Gbauds and a modulation format with higher bit-rate (i.e., PM-16QAM). Moreover, the NETCONF agent acting in the receiver has been extended with a specific NETCONF notification stream, able to provide all the required information to the subscribed clients. In our case the VNFM/VIM performs the subscription to this stream, to receive update once the lightpath is adapted. Indeed, VIM manages the network function virtualisation infrastructure (NFVI) while VNFM manages the virtual network functions.

To further speed up recovery operation, in this study, several vDU and vCU types featuring different functional splits are already installed (i.e., containers

Table III
HOST MACHINES CONFIGURATIONS

Devices Name	Devices Type	Processor Type	OS
Host Machine 1	mini-pc (Up-board First Generation)	Intel Atom x5-Z8350 Quad Core Processor	Ubuntu 14.04 (4.7 kernel)
Host Machine 2	Dell T410 PowerEdge desktop servers	Intel Xeon E5620	Ubuntu 14.04 (3.19 low-latency kernel)
Host Machine 3	Desktop computer (@ 3.60 GHz)	Intel i7 4790 (3.19 low-latency kernel)	Ubuntu 14.04
Host Machine 4	Mini-ITX	Intel I7 7700 Quad Core (@ 4.0GHz)	Ubuntu 14.04 (3.19 low-latency kernel)

```
<state>
  <id>1</id>
  <description>State1</description>
  <events xmlns:ev="http://sssup.it/events">
    <event>
      <name>BER</name>
      <type>ev:ON_CHANGE</type>
      <threshold-param>0.002</threshold-param>
      <check-operator>GT</check-operator>
      <reaction>
        <operation>
          <id>1</id>
          <type>SIMPLE_OP</type>
          <simple>
            <local-address>10.1.1.3</local-address>
            <remote-address>10.1.1.2</remote-address>
            <execute-local>
              <transponder xmlns="http://sssup.it/transponder"
              xmlns:nc="urn:ietf:params:xml:ns:netconf:base:1.0">
                <subcarrier-module>
                  <subcarrier-id>1</subcarrier-id>
                  <config>
                    <bit-rate>112</bit-rate>
                    <baud-rate>28</baud-rate>
                    <modulation xmlns:mf="http://sssup.it/modulation-formats">
                                mf:pm-qpsk
                               </modulation>
                  </config>
                </subcarrier-module>
              </transponder>
            </execute-local>
            <execute-remote>
              <transponder xmlns="http://sssup.it/transponder"
              xmlns:nc="urn:ietf:params:xml:ns:netconf:base:1.0">
                <subcarrier-module>
                  <subcarrier-id>1</subcarrier-id>
                  <config>
                    <bit-rate>112</bit-rate>
                    <baud-rate>28</baud-rate>
                    <modulation xmlns:mf="http://sssup.it/modulation-formats">
                                mf:pm-qpsk
                               </modulation>
                  </config>
                </subcarrier-module>
              </transponder>
            </execute-remote>
            <next-state>2</next-state>
          </simple>
        </operation>
      </reaction>
    </event>
  </events>
</state>
```

Figure 5. Finite state machine configuration

with the respective functions are already allocated) and they are activated upon request. The number of vDUs and vCUs that could be allocated depends on the compute and storage resource of the data centers. As shown in [33], Docker container-based virtualization allows a higher fronthaul latency and jitter budget than virtualization based on virtual machine. Thus Docker container-based virtualization is considered in this experimental evaluation. As shown in Figure 3, *Host Machine 2* contains a Docker with two containers to deploy the two vCUs (i.e., vCU1 and vCU2) with two different functional split options. Here, the vCU1 and vCU2 are used to build and run for Option 8 and Option 7a, respectively. Similarly, the vDU functions with two different functional split options are hosted in *Host Machine 3* (i.e., vDU1 and vDU2) to build and run Option 8 and Option 7a, respectively.

The Ettus Universal Software Radio Peripheral (USRP) B210 device acts as radio front-end performing Digital to Analog and Analog to Digital Conversion (DAC/ADC), Digital Up and Down Conversion (DUC/DAC), low pass filtering and amplification. The USRP B210 is attached to *Host Machine 3*. The Huawei E3372 dongle is utilized as UE. The Huwaei E3372 is capable to transmit 150 Mbps in downlink and 50 Mbps uplink with a signal bandwidth of 20 MHz. The dongle is connected to *Host Machine 4* and connected to the USRP B210 device through SMA cables with a 20 dB of attenuation in the middle of the link.

Table III summarizes the *Host Machines* configurations of the host machines utilized in the scenario depicted in Fig 3. Note that the kernel in *Host Machines* is directly pre-compiled by OAI platform for including the General Packet Radio Service (GPRS) Tunnelling Protocol (GTP) kernel module. The architecture depicted in Figure 1 is implemented in a simplified version. The VIM/VNFM is emulated by a shell script that is triggered by the NFVO when functional split change is required.

The main workflow is highlighted in Fig. 3. At the beginning the VNFM/VIM and the SDN controller perform the setup of the network service, activating vCU1 in host machine 2, vDU1 in host machine 3 and deploying the lightpath interconnecting them (three nodes traversed with modulation 16QAM and baudrate 224Gbauds) with option 8. At step 1, the receiver (RX) detects a value of and consequently the FSM is applied: TX (step 2) and RX (step 3) are reconfigured according to the FSM configuration. Once the reconfiguration is complete, a NETCONF notification is sent (step 4), informing the VNFM/VIM of the lightpath adaptation. Then, the VNFM/VIM performs the activation of vCU2 and vDU2 with option 7a (step 5).

The considered performance evaluation parameter is the *eNB functional split reconfiguration time (FSRT)*, here defined as the time elapsing between the last *ping* reply sent by the EPC to the UE and the detection of the first successive *ping* reply with the requested functional split option at the UE. The FSRT measurement is performed as follows: i) initially, vRAN setup is set to run on vDU1 and vCU1 with functional split Option 8; ii) *ping* is continuously run between the UE and the EPC with packet interval of 1ms; iii) reconfiguration of functional split request command is sent by the VNFM/VIM to vDU2 and vCU2 to initiate the requested functional split (i.e., Option 7a).

IV. Results

A. Simulation results

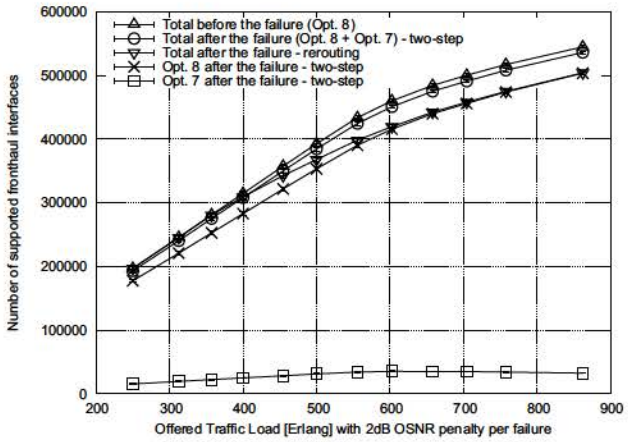

Figure 6. Mean overall recovered rate through transmission parameter adaptation versus offered traffic load, with soft failures introducing an OSNR penalty of 2dB.

Fig. 6 shows the number of supported fronthaul interfaces before and after the soft failure versus the offered traffic load, assuming that each soft failure introduces an OSNR penalty of 2dB. While traffic load increases, with re-routing, the lack of available network resources on alternate paths causes the fail of lightpath re-routing, thus several fronthaul interfaces are not supported anymore. Conversely, the proposed two-step scheme exploits lightpath adaptation along the same route and the change of modulation format makes feasible the transmission even with the OSNR degradation, thus recovery is not blocked for lack of network resources and two-step recovery outperforms re-routing. The plot also shows the number of supported Option 8 and Option 7 interfaces after the failure in the case of two-step recovery. The former belongs to the lightpaths which are not impacted by the soft failure. At high loads, re-routing approaches the Option 8 interfaces with two-steps because all lightpath re-routings are blocked for lack of resources, thus only Option 8 traffic not impacted by the failure is present in the network. The number of supported Option 7 interfaces after the failure slightly increases with load because more lightpaths are impacted the soft failure, thus the change of functional split is more likely exploited.

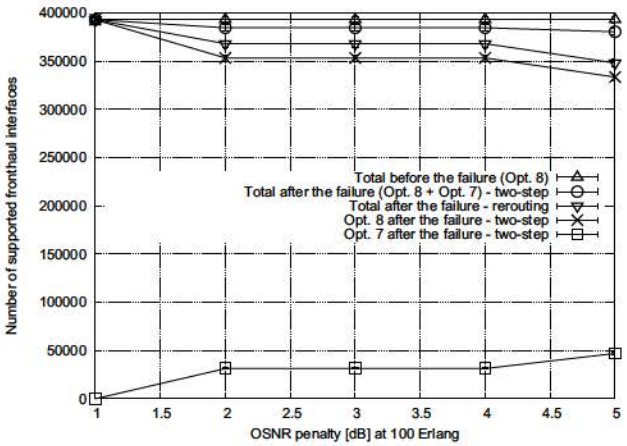

Figure 7. Mean overall recovered rate through transmission parameter adaptation versus soft-failure OSNR penalty, with a traffic load of 100 Erlang.

Fig. 7 shows the number of supported fronthaul interfaces before and after the soft failure versus the OSNR penalty with a traffic load of 500 Erlang. The total number of supported interfaces after failure decreases with the OSNR penalty. Indeed, the number of lightpaths impacted by the soft failure increases with the OSNR penalty because the larger the penalty the higher the probability of passing the BER threshold of 10^{-3}. Thus, in the case of re-routing, more lightpaths contends available network resources on alternate paths, while, in the case of two-step recovery, more lightpaths must rely on bit rate reduction.

B. Experimental results

Table IV shows the average values of overall transport network reconfiguration time in the considered scenario for lightpath adaption. The value of *TX reconf* reports the time required to reconfigure the TX. The value of the *RX reconf* indicates the time required for both TX and RX reconfiguration. Then, the value at the *NETCONF notify* is the overall time required for the reconfiguration, including the NETCONF notification to the VNFM/VIM related to the lightpath adaptation. Two different lightpath adaption scenarios are considered such as: (i) from high bit rate to low bit rate (i.e., from 16QAM/32Gbauds to QPSK/28Gbauds); ii) from low bit rate to high bit rate (i.e., from QPSK/28Gbauds to 16QAM/32Gbauds). These two different scenarios are based on the pre-defined parameters as show in Fig. 3. The overall transport network reconfiguration from high bit rate to low bit rate is around 295ms, while from the low bit rate to high bit rate is around 316ms as shown in the Tab. IV.

Upon receiving the NETCONF notification about the lightpath adaptation as shown in Fig. 3, the VNFM/VIM performs the activation of vCU2 and

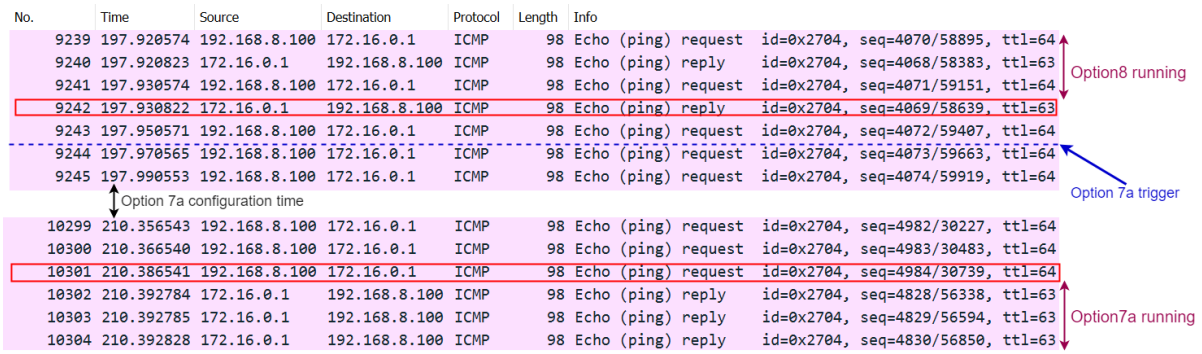

Figure 8. Capture, at the UE, of ICMP messages exchanged between the UE and the EPC.

Table IV
TRANSPORT NETWORK RECONFIGURATION TIME

Lightpath adaption	TX reconf time [ms]	RX reconf time [ms]	NETCONF notify time [ms]
From high bit rate to low bit rate	145.83	250.39	294.51
From low bit rate to high bit rate	166.75	272.83	315.64

vDU2 with option 7a. Fig. 8 illustrates the wireshark capture of *ping* messages at the UE during the eNB functional split reconfiguration. The ping messages (i.e., ICMP request and reply messages) are exchanged between the UE (dongle), whose IP address is 192.168.8.1, and the EPC, whose GTP interface IP address is 172.16.0.1. Notice that the vRAN setup is established and running with functional split Option 8, initially. The timestamp of the wireshark is measured in seconds. As shown in Fig. 8, the last ICMP reply message is received by the UE at timestamp 197.930822 s before functional split Option 7a is triggered. Upon functional split reconfiguration is triggered, only ICMP request messages at the UE can be observed. The first successive ICMP reply message from the EPC to the UE is received at timestamp 210.392784 s, showing the successful reconfiguration of the functional split Option 7a. Thus, the time elapsing between the last ICMP reply message and the first successive ICMP reply message at the UE (i.e., the FSRT) is about 12 s. This obtained FSRT values also includes a 2 s sleep time to synchronize the fronthaul interface between OAI DU and OAI CU during Option 7a configuration, and the shell-based VIM controller contribution of about 1 s to enter into the containers to run the requested functional split option.

V. CONCLUSIONS

This paper proposed a two-step scheme for recovering virtualised distributed unit (vDU) and virtualised central unit (vCU) connectivity upon fronthaul failure. In particular, a single soft failure of a lightpath interconnecting vCU and vDU is considered. The main novelty of the proposed scheme consists of complementing lightpath adaptation with the possibility of flexibly changing the vCU and vDU functional split. This approach allows to increase the number of recovered connections when network spare resources are scarce.

Simulation results showed that the proposed scheme allows to recover almost all the fronthaul vDU-vCU connections along the same path where working lightpaths were routed and it largely overcomes the performance of lightpath rerouting, specially when the network load is high. Experimental results showed that the recovery time experienced when functional split change is triggered is in the order of tens of seconds.

ACKNOWLEDGMENT

This work was partly funded by the project H2020-ICT-2016-2 “5G-TRANSFORMER” (761536)

REFERENCES

[1] J. Zou, C. Wagner, and M. Eiselt, “Optical fronthauling for 5G mobile: A perspective of passive metro WDM technology,” in *2017 Optical Fiber Communications Conference and Exhibition (OFC)*, March 2017, pp. 1–3.

[2] G. N. Liu, L. Zhang, T. Zuo, Q. Zhang, J. Zhou, and E. Zhou, “IM/DD transmission techniques for emerging 5G fronthaul, DCI and metro applications,” in *2017 Optical Fiber Communications Conference and Exhibition (OFC)*, March 2017, pp. 1–3.

[3] V. Passas, V. Miliotis, N. Makris, T. Korakis, and L. Tassiulas, “Paris metro pricing for 5G HetNets,” in *2016 IEEE Global Communications Conference (GLOBECOM)*, Dec 2016, pp. 1–6.

[4] F. Musumeci, M. Tornatore, and A. Pattavina, “A techno-economic outlook to optical interface requirements for mid-hauling of 5G small cells,” in *ECOC 2016; 42nd European Conference on Optical Communication*, Sep. 2016, pp. 1–3.

[5] Y. Pointurier, “Design of low-margin optical networks,” *IEEE/OSA Journal of Optical Communications and Networking*, vol. 9, no. 1, pp. A9–A17, Jan 2017.

[6] N. Sambo, F. Cugini, A. Sgambelluri, and P. Castoldi, “Monitoring plane architecture and OAM handler,” *Journal of Lightwave Technology*, vol. 34, no. 8, April 2016.

[7] A. Dupas, P. Layec, E. Dutisseuil, S. Bigo, S. Belotti, S. Misto, S. Annoni, Y. Yan, E. Hugues-Salas, G. Zervas, and D. Simeonidou, "Hitless 100 Gbit/s OTN bandwidth variable transmitter for software-defined networks," in *2016 Optical Fiber Communications Conference and Exhibition (OFC)*, March 2016, pp. 1–3.

[8] P. Layec, A. Dupas, A. Bisson, and S. Bigo, "QoS-aware protection in flexgrid optical networks," in *2017 Optical Fiber Communications Conference and Exhibition (OFC)*, March 2017, pp. 1–3.

[9] 5G PPP, "View on 5G architecture," White Paper, https://5g-ppp.eu/white-papers (accessed August 10, 2018).

[10] A. Checko, H. L. Christiansen, Y. Yan, L. Scolari, G. Kardaras, M. S. Berger, and L. Dittmann, "Cloud RAN for mobile networks – a technology overview," *IEEE Communications Surveys Tutorials*, vol. 17, no. 1, pp. 405–426, First Quarter 2015.

[11] J. X. Salvat, A. Garcia-Saavedra, X. Li, and X. Costa-Perez, "WizHaul: An automated solution for vRAN deployments optimization," in *WSA 2018; 22nd International ITG Workshop on Smart Antennas*, March 2018, pp. 1–7.

[12] 3rd Generation Partnership Project; Technical Specification Group Radio Access Network, "Study on new radio access technology; radio access architecture and interfaces," 3GPP TR 38.801 V2.0.0 (2017-03).

[13] "Next generation fronthaul interface (1914) working group," http://sites.ieee.org/sagroups-1914 (accessed August 10, 2018).

[14] Common Public Radio Interface Specification (eCPRI) V1.0. [Online] Available: http://www.cpri.info/spec.html, Tech. Rep., 2017.

[15] L. Valcarenghi, K. Kondepu, and P. Castoldi, "Time- versus size-based cpri in ethernet encapsulation for next generation reconfigurable fronthaul," *J. Opt. Commun. Netw.*, vol. 9, no. 9, pp. D64–D73, Sep 2017.

[16] ITU-T Technical Report Telecommunication Standardization Sector of ITU (9 February 2018) GSTR-TN5G Transport network support of IMT-2020/5G. [Online] Available: https://www.itu.int/dms_pub/itu-t/opb/tut/T TUT-HOME-2018-PDF-E.pdf, Tech. Rep., 2017.

[17] K. Kondepu, N. Sambo, F. Giannone, P. Castoldi, and L. Valcarenghi, "Orchestrating lightpath adaptation and flexible functional split to recover virtualized RAN connectivity," in *2018 Optical Fiber Communications Conference and Exhibition (OFC)*, 2018.

[18] M. R. Rahman and R. Boutaba, "SVNE: Survivable virtual network embedding algorithms for network virtualization," *IEEE Transactions on Network and Service Management*, vol. 10, no. 2, pp. 105–118, June 2013.

[19] F. Gu, H. Alazemi, A. Rayes, and N. Ghani, "Survivable cloud networking services," in *2013 International Conference on Computing, Networking and Communications (ICNC)*, Jan 2013, pp. 1016–1020.

[20] L. Valcarenghi, F. Cugini, F. Paolucci, and P. Castoldi, "Quality-of-service-aware fault tolerance for grid-enabled applications," *Optical Switching and Networking*, vol. 5, no. 2, pp. 150 – 158, 2008, advances in IP-Optical Networking for IP Quad-play Traffic and Services.

[21] R. Tucker, M. Ruffini, L. Valcarenghi, D. R. Campelo, D. Simeonidou, L. Du, M.-C. Marinescu, C. Middleton, S. Yin, T. Forde, K. Bourg, E. Dai, E. Harstead, P. Chanclou, H. Roberts, V. Jungnickel, S. Figuerola, T. Takahara, R. Yadav, P. Vetter, D. A. Khotimsky, and J. S. Wey, "Connected OFCity: Technology innovations for a smart city project (invited)," *J. Opt. Commun. Netw.*, vol. 9, no. 2, pp. A245–A255, Feb 2017.

[22] ETSI, "Network functions virtualisation (nfv); management and orchestration," ETSI GS NFV-MAN 001 v1.1.1 (2014-12).

[23] E. Riccardi, P. Gunning, O. de Dios, M. Quagliotti, V. Lopez, and A. Lord, "An operator view on the introduction of white boxes into optical networks," *Journal of Lightwave Technology*, vol. 36, no. 15, pp. 3062–3072, Aug 2018.

[24] G. Agrawal, "Fiber-optic communication systems," *Wiley-Interscience Publication*, 1997.

[25] G. Bosco, V. Curri, A. Carena, P. Poggiolini, and F. Forghieri, "On the performance of Nyquist-WDM Terabit superchannels based on PM-BPSK, PM-QPSK, PM-8QAM or PM-16QAM subcarriers," *JLT*, 2011.

[26] N. Sambo, M. Secondini, F. Cugini, G. Bottari, P. Iovanna, F. Cavaliere, and P. Castoldi, "Modeling and distributed provisioning in 10-40-100-Gb/s multirate wavelength switched optical networks," *Journal of Lightwave Technology*, vol. 29, no. 9, pp. 1248–1257, May 2011.

[27] L. Valcarenghi, F. Giannone, D. Manicone, and P. Castoldi, "Virtualized eNB latency limits," in *19th International Conference on Transparent Optical Networks (ICTON)*, July 2017, pp. 1–4.

[28] OpenAirInterface (OAI), "Openairinterface source code for next generation cellular standard," http://www.openairinterface.org (accessed 20/09/2017).

[29] OpenAirInterface (openair-cn), "An implementation of the evolved packet core network," https://gitlab.eurecom.fr/oai/openair-cn (accessed 20/09/2017).

[30] K. Christodoulopoulos and at al., "Observe-decide-act: Experimental demonstration of a self-healing network," in *2018 Optical Fiber Communications Conference and Exhibition (OFC)*, 2018.

[31] M. Dallaglio, N. Sambo, F. Cugini, and P. Castoldi, "YANG models for vendor-neutral optical networks, reconfigurable through state machine," *IEEE Communications Magazine*, vol. 55, no. 8, pp. 170–178, 2017.

[32] N. Sambo, A. Giorgetti, F. Cugini, and P. Castoldi, "Sliceable transponders: Pre-programmed OAM, control, and management," *Journal of Lightwave Technology*, vol. 36, no. 7, pp. 1403–1410, April 2018.

[33] H. Gupta, D. Manicone, F. Giannone, K. Kondepu, A. Franklin, P. Castoldi, and L. Valcarenghi, "How much is fronthaul latency budget impacted by RAN virtualisation ?" in *2017 IEEE Conference on Network Function Virtualization and Software Defined Networks (NFV-SDN)*, Nov 2017, pp. 1–6.